Torsional lag in wide flanged girders

Torsional Lag in Wide Flanged Girders

Traînage de torsion dans les poutres à semelle large

Torsionsverzerrungen in Breitflanschträgern

Patrick J. DOWLING
Prof. of Steel Structures
Imperial College
London, UK

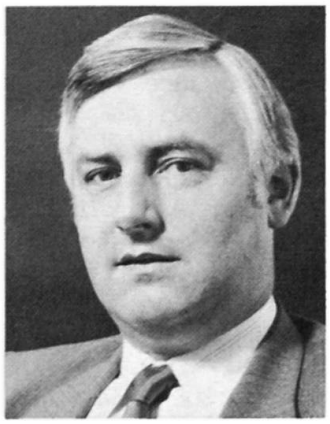

P.J. Dowling is Head of the Civil Engineering Department at Imperial College and director of the consulting firm Chapman, Dowling and Associates. He is Chairman of the Eurocode 3 (Steel Structures) Drafting Panel for the EEC.

Bassam A. BURGAN
Research Student
Imperial College
London, UK

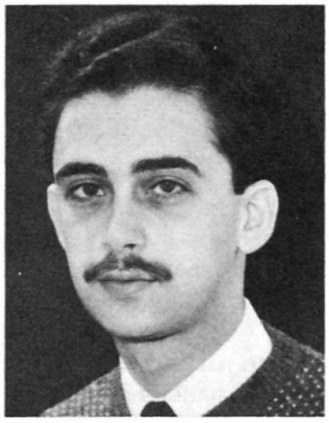

B.A. Burgan graduated in 1982 as a Civil Engineer from the University of Salford. In 1983 he obtained his MSc and DIC from Imperial College in Structural Steel Design. Currently, he is researching into the behaviour of plate and box girders.

SUMMARY

The paper presents a study of torsional lag in wide flange girders. The influence of a number of parameters is examined. A torsional lag effective with definition is suggested. Simple expressions are derived to enable the bending moment at any point in the flange to be calculated. It was found that torsional lag can affect the position of maximum stress across the flange and this helps explain some experimentally observed modes of failure.

RÉSUMÉ

Ce mémoire présente une étude du phénomène de traînage de torsion dans les poutres à semelle large. L'influence d'un certain nombre de paramètres est examinée. Une définition de la largeur efficace de traînage de torsion est proposée. Des formules simples, permettant de déterminer le moment fléchissant en différents points de la semelle, sont développées. Aussi, il a été observé que la zone de contrainte maximale est affectée par le traînage de torsion, ce qui explique, en grande partie, certains modes de ruine observés expérimentalement.

ZUSAMMENFASSUNG

Der Beitrag enthält eine Untersuchung der Torsionsverzerrungen in Breitflanschträgern, wobei der Einfluss mehrerer Parameter studiert wurde. Eine mitwirkende Flanschbreite, welche die Torsionsverzerrungen berücksichtigt, wird eingeführt. Einfache Formeln zur Berechnung des Biegemomentes in beliebigen Punkten des Flansches werden abgeleitet. Es wurde festgestellt, dass die Position der Maximalspannung im Flansch durch die Schubverzerrung beeinflusst werden kann, was einige experimentell festgestellte Bruchverhalten erklärt.

1. INTRODUCTION

Recent research on the interaction between buckling and shear lag has shown that in the case of stiffener-induced buckling, a number of different phenomena interact to produce the final failure mode [1,2]. These observations were based mainly on experimental work with some attempts at numerically modelling such a mode of failure. The phenomena were classified as:

(a) shear lag,
(b) the column P-Δ effect
(c) a 'bending lag', and
(d) anticlastic curvature.

This paper addresses the third of the above effects but also incorporates the fourth. Reference to 'bending lag' can be traced back to 1971 [3] where it was called 'bending reluctance' of the flange. By analogy with shear lag (which arises due to the finite in-plane shear stiffness of a plate), 'bending lag', arises as a result of the finite torsional stiffness of a plate. It is for this reason that in the remainder of this work it will be referred to as torsional lag. Torsional lag is manifested in the tendency of the longitudinal curvature of a flange plate to diminish with increasing distance from the web.

The phenomenon of torsional lag would be important, for example, in shallow box girders with wide stiffened flanges such as are occasionally used in bridge and offshore construction. In such girders, flange failure can be initiated at a point remote from the flange edges due to the interaction of all the phonemena listed above. An understanding of the influence of torsional lag is necessary to explain such a mode of failure.

The double-webbed plate girder shown in figure 1 is considered. It is assumed to be simply supported and the loads are assumed to be applied to the webs. The differential equation for small deflections is solved analytically using trigonometric-hyperbolic series. The loads are modelled using Fourier series. The analysis considers the effect of a number of parameters including the aspect ratio, type of loading, degree of orthotropy and the main girder stiffness.

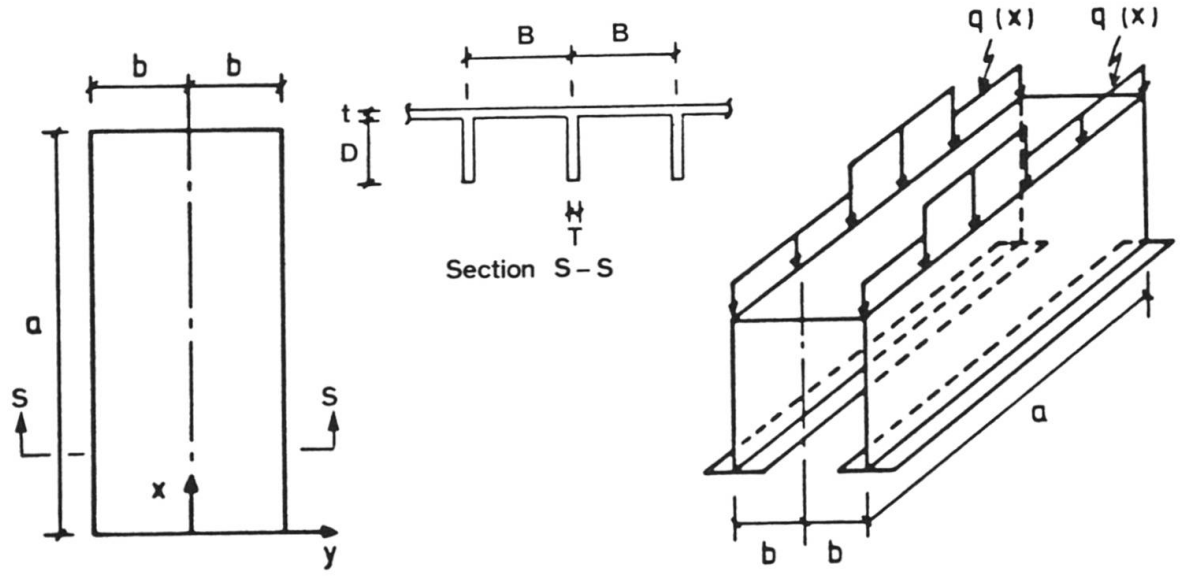

Fig. 1 Girder under consideration with plan view showing flange dimensions and axis. The longitudinal stiffener dimensions are also shown.

We consider the simplest case of a flange with no initial imperfections, yielding or residual stresses in order to provide an understanding of torsional lag without the interaction of other effects which would complicate the issue; such interaction will be considered in future work. In-plane forces due to overall bending of the girder and their effect on the behaviour of the flange are also not considered here, thus leaving bending stresses only. In this way we can show how the plate behaves when a curvature is applied to its edges.

The analysis gives rise to two possible definitions of torsional lag effective width, one based on longitudinal curvatures and the other on longitudinal moments. These are considered in order to select an appropriate effective width.

2. BOUNDARY CONDITIONS

2.1 Support Conditions x=0,a

The girder ends are assumed to be simply supported. Thus the edges are assumed to rotate out of their plane independently of the supports. The simple support assumption also provides for zero vertical displacement of the edges of the compression flange. The out-of-plane boundary conditions can thus be written

$$w = 0 \tag{2.1}$$

$$\frac{\partial^2 w}{\partial x^2} = 0 \tag{2.2}$$

2.2 Web-flange junction conditions y=+b,-b

The flexibility of the web is taken such that it is reasonable to assume rotations in the transverse direction independent of the web hence resulting in zero transverse moment. The edges deflect to follow the vertical displacement of the web. The out-of-plane boundary conditions can thus be expressed

$$M_y = -D_y \frac{\partial^2 w}{\partial y z} - D_1 \frac{\partial^2 w}{\partial x^2} = 0 \tag{2.3}$$

$$-D_y \frac{\partial^3 w}{\partial y^3} - (D_1 + 4D_{xy}) \frac{\partial^3 w}{\partial x^2 \partial y} + EI \frac{\partial^4 w}{\partial x^4} - q(x) = 0 \tag{2.4}$$

3. DETERMINATION OF PLATE RIGIDITIES

The torsional lag effective width was found to be sensitive to the variation in plate rigidities and the way in which they are calculated. Little is available in the literature on the accurate theoretical determination of plate rigidities for eccentrically stiffened plates. Most of the work done in this area replaces the plate/stiffener combination by an "equivalent" homogeneous orthotropic plate of constant thickness and then applies orthotropic plate theory to the plate/stiffener combination. For such an approximation to be applicable, the ratio of stiffener spacing to plate dimensions should be small (B/b, B/a << 1).

The flange plate here is assumed to be stiffened in the longitudinal x-direction only. The plate rigidities were calculated using the following approximate expressions:

$$D_x = \frac{Et^3}{12(1-\nu_x\nu_y)} + \frac{Eth^2}{(1-\nu_x\nu_y)} + \frac{EI_s}{B} \qquad D_y = \frac{Et^3}{12(1-\nu_x\nu_y)} \tag{3.1}$$

$$E_x = \frac{E(DT+Bt)}{Bt} \qquad E_y = E \qquad \nu_x = \nu \qquad \nu_y = \frac{\nu Bt}{(DT+Bt)}$$

$$G_{xy} = \frac{\sqrt{E_x E_y}}{2(1+\sqrt{\nu_x \nu_y})} \qquad D_{xy} = \frac{G_{xy} t^3}{12} + \frac{G_{xy} J}{4B} \qquad D_1 = \frac{\nu E t^3}{12(1-\nu^2)}$$

$$H = D_1 + 2D_{xy}$$

In such cases where the orthotropy is caused by structural form, it may be difficult to comply with Betti's reciprocal theorem and careful consideration is required when evaluating rigidities, especially D_1.

4. CALCULATION OF TORSIONAL LAG EFFECTIVE WIDTH

To provide an easy means of quantifying torsional lag and the way in which it is affected by the various parameters of the problem, it is convenient to define a torsional lag effective width. Two ways in which such an effective width can be defined are considered here.

(a) Effective width based on the distribution of longitudinal curvature across the width (i.e. the variation of $\partial^2 w/\partial x^2$ with y). Mathematically, this can be written as follows:

$$b_e = \frac{\int_0^b \partial^2 w/\partial x^2 \, dy}{[\partial^2 w/\partial x^2]_{y=b}} \qquad (4.1)$$

Hence no account is taken of the anticlastic curvature and the definition gives the effective width which would sustain a constant longitudinal curvature across the width equal to the maximum curvature. Substitution of the derivatives of w into the above definition gives three expressions for the effective width for:

$H^2 > D_x D_y$
$H^2 = D_x D_y$
$H^2 < D_x D_y$

(b) Effective width based on the distribution of longitudinal moments across the width (i.e. the variation of M_x with y at a given cross-section). Mathematically, this can be written as follows:

$$b_e = \frac{\int_0^b M_x dy}{[M_x]_{y=b}} \qquad (4.2)$$

In this case the effective width is that width of plate which would sustain a constant bending moment equal to the actual moment in the plate. Substitution of the derivatives of w into the above definition yields three expressions for the effective width for:

$H^2 > D_x D_y$
$H^2 = D_x D_y$
$H^2 < D_x D_y$

It can be seen that due to the presence of an anticlastic curvature the effective width values obtained from the first definition will be slightly higher than those obtained from the second. From the viewpoint of both analysis and design, we are mainly interested in the moment and not the curvature that the section can sustain and thus it seems more logical to adopt the second definition. This has been done in the remainder of this work as the first does not give an effective section in the usual sense.

The concept of a torsional lag effective width is illustrated in figure 2. The torsional lag effective width ratio β is then defined as b_e/b.

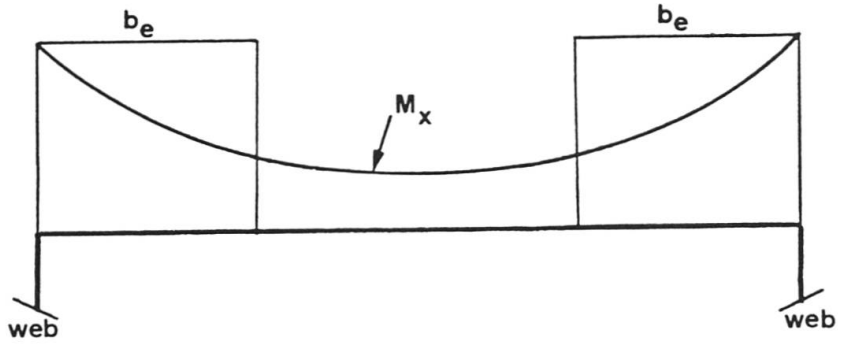

Fig. 2 The torsional lag effective width concept.

5. PARAMETERS INFLUENCING TORSIONAL LAG

5.1 Aspect ratio

As in the case of shear lag, the aspect ratio was found to be one of the most important parameters influencing torsional lag. The importance of this parameter can be seen in figure 2 which shows plots of effective width at mid-span vs aspect ratio (b/a) for three different degrees of stiffening and under a centrally applied point load. The curves can be seen to be similar to those in the shear lag literature.

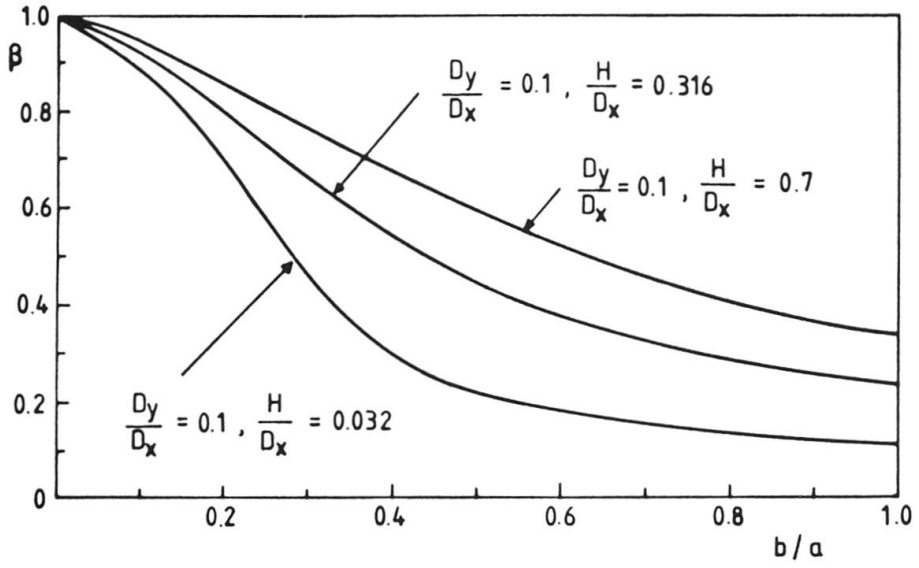

Fig. 3 Variation of effective width with aspect ratio.

5.2 Degree of orthotropy

The amount of stiffening was found to be a very important parameter in influencing torsional lag. Unlike shear lag where it was sufficient to specify the ratio of stiffener to plate areas per unit width of plate, it is necessary here to specify the flexural characteristics of the stiffener/plate combination. The torsional rigidity H was found to be the most important orthotropy parameter governing torsional lag. The effect of the transverse flexural rigidity is not negligible as it enters into the calculation of the

torsional rigidity. Figure 3 shows the effect of orthotropy for three aspect ratios. The effective width is evaluated at mid-span under a point load. The important effect of the degree of orthotropy is clearly apparent from this figure.

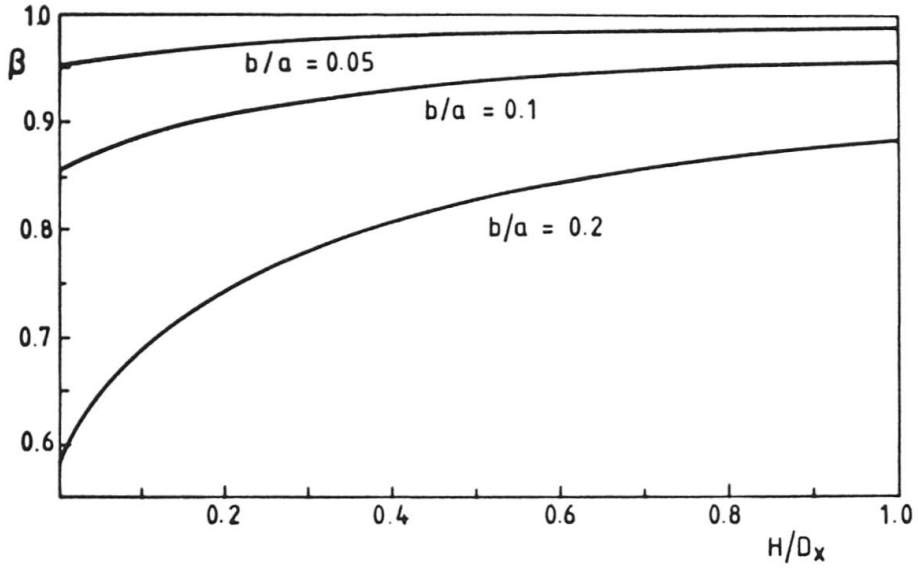

Fig. 4 Variations of effective width with torsional rigidity.

5.3 Web stiffness

The effect of web stiffness can be measured using the non-dimensional parameter $(EI/D_x a)$. This effect was found to be very small in the central range of $(EI/D_x a)$, and negligible outside this range, as can be seen from figure 4 for three different aspect ratios. A point load at mid-span is assumed. These curves seem to take the shape of a very flat S. It is important to note here that the web stiffness has a very marked effect on the magnitude of the moment in the flange.

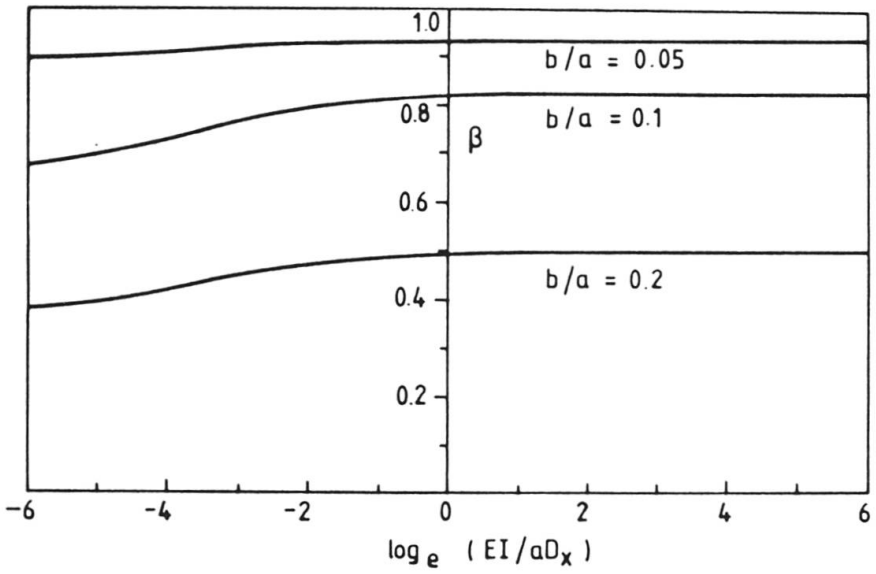

Fig. 5 Variation of effective width with web stiffness.

5.4 Type of loading

The distribution of applied load on the girder has a significant effect on the torsional lag effective width in the same way as is the case with shear lag. Two types of loading were considered here; a centrally applied point load and a uniformly distributed load. The point load results in the most pronounced torsional lag effect. Figure 5 shows the variation of torsional lag effective width with aspect ratio for the two types of loading. This is shown for an isotropic and an orthotropic plate.

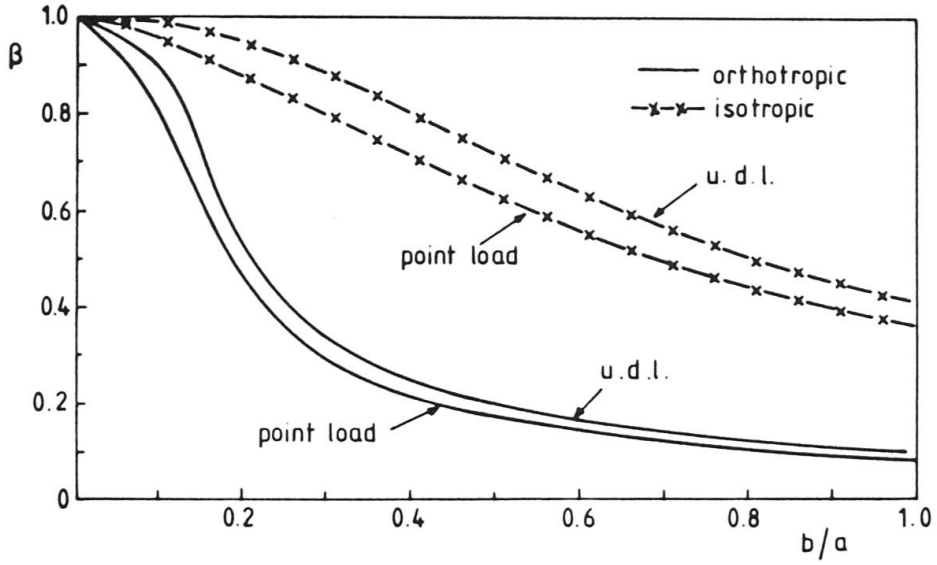

Fig. 6 Variation of effective width with type of loading.

6. DISTRIBUTION OF LONGITUDINAL BENDING MOMENT ACROSS THE WIDTH

The availability of a torsional lag effective width enables the peak bending moment in the flange at the web-flange junction M_{max} to be calculated. However, tests on plate girders in which failure was induced by stiffener buckling [1,2] have shown that the first stiffeners to fail were those situated at about the quarter width. It is therefore necessary to have an estimate of the longitudinal bending moment in parts of the flange remote from the web-flange junction. These moments may be obtained using the following formulae:

$$M_x = M_{max}\left[1.35\beta-0.36-(0.63\beta-0.73)\left[\frac{y}{b}\right]^2-(0.62\beta-0.61)\left[\frac{y}{b}\right]^4\right] \quad \text{for } \beta > 0.225 \quad (6.1)$$

$$M_x = M_{max}\left[-0.71\beta+0.10+(9.26\beta-1.62)\left[\frac{y}{b}\right]^2-(6.96\beta-2.22)\left[\frac{y}{b}\right]^4\right] \quad \text{for } \beta \leq 0.225 \quad (6.2)$$

Figure 6 shows a comparison between the distributions of longitudinal moment obtained from these approximate expressions and those obtained from the closed form solution. The agreement can be seen to be excellent. Slight inaccuracies arise, however, for very small values of effective width ($\beta < 0.1$) but these usually fall outside the practical range.

The magnitude of the bending moment in the flange under the assumed loading conditions is very sensitive to variation in the web stiffness; the greater the web stiffness, the smaller the longitudinal moment in the plate and for nearly all practical web sizes is very small. However, at ultimate load the effect of such a moment distribution is not insignificant as it will be exaggerated by the P-Δ effect, large deflections and the

presence of imperfections. The combination will initiate a failure at a location remote from the web for certain geometries and indeed this is what happened in the test model of references [1,2].

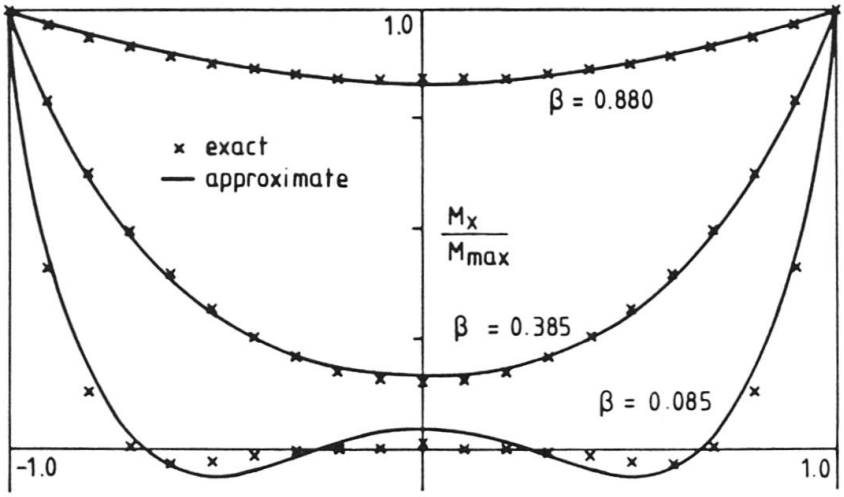

Fig. 7 Comparison between the exact and approximate expressions for the distribution of bending moment across the flange.

Given that the web provides no rotational restraint to the flange, a simple expression may be derived for the maximum bending moment (i.e. at the web/flange junction) by considering the overall equilibrium of the girder and making use of the torsional lag effective width. This is given by:

$$M_{max} = \frac{(1-D_1^2/D_xD_y)M}{2\left[\frac{EI}{D_x} + b_e(1-D_1^2/D_xD_y)\right]} \qquad (6.3)$$

It is then possible by using expressions (6.1) or (6.2) to calculate the flange bending moment at any point.

7. CONCLUSION

The paper has presented for the first time a comprehensive study of the phenomenon of torsional lag. The case of an elastic flat orthotropic plate forming the flange of a girder was used for the purposes of this study. The way in which a proper understanding of torsional lag can help explain some experimental observations has been discussed. In the case of flange failure by stiffener-induced buckling, torsional lag is thought to be of particular importance in explaining the observed mode of failure.

A definition of torsional lag effective width has been suggested as a means of quantifying torsional lag. The effect of the aspect ratio, the degree of orthotropy, the type of loading and the web stiffness was studied. It was found that the torsional lag effective width was sensitive to the first three parameters while variations in web stiffness had a negligible effect when the latter was greater than the flange stiffness, as is usually the case. The degree of orthotropy needs to be measured in terms of the rigidities of the plate and not simply as the ratio of stiffener to plate areas. The orthotropy parameter of interest was found to be H/D_x.

Shear lag effective width is used in conjunction with the overall bending of the girder with the flange acting as a compression or tension member. By contrast, the torsional lag effective width is used in conjunction with the bending of the flange plate itself (together with any stiffeners); i.e., the flange is acting as a bending member when considering torsional lag.

The way in which the torsional lag effective width is applied in the analysis was demonstrated. Simple expressions for the evaluation of the longitudinal bending moment at any point across the flange have been given.

APPENDIX

Solution of the governing differential equation

The small deflection differential equation of an orthotropic plate in bending is

$$D_x \frac{\partial^4 w}{\partial x^4} + 2H \frac{\partial^4 w}{\partial x^2 \partial y^2} + D_y \frac{\partial^4 w}{\partial y^4} = q(x,y) \qquad (A.1)$$

and if only edge loading is applied the equation reduces to its homogeneous form

$$D_x \frac{\partial^4 w}{\partial x^4} + 2H \frac{\partial^4 w}{\partial x^2 \partial y^2} + D_y \frac{\partial^4 w}{\partial y^4} = 0 \qquad (A.2)$$

the general solution takes the form

$$w = \sum_{m=1}^{\infty} F(y) \sin \frac{m\pi x}{a} \qquad (A.3)$$

and substitution of this into the governing differential equation results in the following characteristic equation

$$D_x \left[\frac{m\pi}{a}\right]^4 F(y) - 2H \left[\frac{m\pi}{a}\right]^2 F''(y) + D_y F''''(y) = 0 \qquad (A.4)$$

where a' denotes differentiation with respect to y.

The roots of this equation depend on the relationship between D_x, D_y and H and three situations arise:

1. $H^2 > D_x D_y$ for a torsionally stiff and/or flexurally soft bridge deck
2. $H^2 = D_x D_y$ for an isotropic bridge deck
3. $H^2 < D_x D_y$ for a torsionally soft and/or flexurally stiff bridge deck

Symmetry of the plate geometry and its loading requires the solution to be an even function of y and this reduces the number of unknown constants from four to two.

The boundary conditions at the edges x = 0,a are satisfied by the choice of solution while the other two boundary conditions at the web/flange junction are used to determine the constants in the general solution. The three cases give three different solutions and these are presented here.

Case 1. $H^2 > D_x D_y$

The roots of the characteristic equation in this case are all real and are given by

$$\alpha_{1,2,3,4} = \pm \frac{m\pi}{a} \sqrt{\frac{1}{D_y} (H \pm \psi)} = \frac{m\pi}{a} r_{1,2,3,4} \qquad (A.5)$$

where $\psi = \sqrt{H^2 - D_x D_y}$

and hence the deflection surface is given by

$$w = \sum_{m=1}^{\infty} \sin \frac{m\pi x}{a} (A_1 \cosh\alpha_1 y + A_2 \cosh\alpha_2 y) \qquad (A.6)$$

The condition that $M_y = 0$ at $y = b$ gives the relationship between A_2 and A_1:

$$A_1 = \frac{\cosh\alpha_2 b \, (\psi - 2D_{xy})}{\cosh\alpha_1 b (\psi + 2D_{xy})} A_2 \qquad (A.7)$$

and the second condition of equilibrium of the edge gives A_2 in terms of the known parameters of the problem which reduces to

$$A_2 \left[\frac{m\pi}{a}\right]^3 \sin \left[\frac{m\pi x}{a}\right] \left[-r_1 \frac{(\psi - 2D_{xy})^2}{(\psi + 2D_{xy})} \cosh\alpha_2 b \tanh\alpha_1 b \right.$$
$$\left. + r_2 (\psi + 2D_{xy}) \sinh\alpha_2 b + \frac{2\psi}{(\psi + 2D_{xy})} EI \frac{m\pi}{a} \cosh \alpha_2 b \right] - q(x) = 0 \qquad (A.8)$$

This gives the deflected surface of the plate on substituting back into the expression for w.

Case 2. $H^2 = D_x D_y$

The differential equation in this case has two roots:

$$\alpha = \pm \frac{m\pi}{a} \sqrt{\frac{H}{D_y}} = \pm \frac{m\pi}{a} r \qquad (A.9)$$

The deflection surface then takes the form

$$w = \sum_{m=1}^{\infty} \sin \left[\frac{m\pi x}{a}\right] \left[A_1 \cosh\alpha y + A_2 \frac{m\pi y}{a} \sinh\alpha y\right] \qquad (A.10)$$

The condition that $M_y = 0$ at $y = b$ gives the relationship between A_2 and A_1:

$$A_1 = A_2 \left[\frac{2D_y}{(D_1 - D_y)} - \frac{m\pi b}{a} \tanh\alpha b\right] = B_1 A_2 \qquad (A.11)$$

and the second condition of equilibrium of the edge gives A_2 in terms of the known parameters of the problem which reduces to

$$A_2\left[\frac{m\pi}{a}\right]^3 \sin\left[\frac{m\pi x}{a}\right]\left[-D_y r^3\left(B_1\sinh\alpha b + \frac{3}{r}\sinh\alpha b + \frac{m\pi b}{a}\cosh\alpha b\right)\right.$$

$$+ (D_1 + 4D_{xy})r\left(B_1\sinh\alpha b + \frac{1}{r}\sinh\alpha b + \frac{m\pi b}{a}\cosh\alpha b\right) \qquad (A.12)$$

$$\left. + \frac{2D_y}{D_1 - D_y} EI \frac{m\pi}{a}\cosh\alpha b\right] - q(x) = 0$$

This gives the deflected surface of the plate on substituting back into the expression for w.

Case 3. $H^2 < D_x D_y$

The roots of the characteristic equation in this case are imaginary and are given by

$$\alpha_{1,2,3,4} = \pm\frac{m\pi}{a}\sqrt{\frac{H}{D_y} \pm \frac{\sqrt{H^2 - D_x D_y}}{D_y}} = \pm\frac{m\pi}{a}\sqrt{\frac{H}{D_y} \pm i\sqrt{\frac{D_x}{D_y} - \frac{H^2}{D_y^2}}}$$

$$= \pm(\eta \pm i\xi) \qquad (A.13)$$

where $\eta = \frac{m\pi}{a}\sqrt{\frac{1}{2}\left[\sqrt{\frac{D_x}{D_y}} + \frac{H}{D_y}\right]} = \frac{m\pi r_1}{a}$; $\xi = \frac{m\pi}{a}\sqrt{\frac{1}{2}\left[\sqrt{\frac{D_x}{D_y}} - \frac{H}{D_y}\right]} = \frac{m\pi r_2}{a}$

and hence using the trigonometric representation of complex numbers, the deflection surface is given by

$$w = \sum_{m=1}^{\infty} \sin\left[\frac{m\pi x}{a}\right](A_1\cosh\eta y\cos\xi y + A_2\sinh\eta y\sin\xi y) \qquad (A.14)$$

The condition that $M_y = 0$ at $y = b$ gives the relationship between A_2 and A_1:

$$A_1 = \frac{\sqrt{D_x D_y - H^2}\cos\xi b + 2D_{xy}\tanh\eta b\sin\xi b}{\sqrt{D_x D_y - H_2}\tanh\eta b\sin\xi b - 2D_{xy}\cos\xi b} A_2 = B_1 A_2 \qquad (A.15)$$

and the second condition of equilibrium of the edge gives A_2 in terms of the known parameters of the problem which reduces to

$$A_2\left[\frac{m\pi}{a}\right]^3 \sin\left[\frac{m\pi x}{a}\right]\cosh\eta b\left\{\left[\sqrt{D_x D_y}\,(B_1 r_1 - r_2) - D_1(B_1 r_1 + r_2)\right]\tanh\eta b\cos\xi b\right.$$

$$+\left[\sqrt{D_x D_y}\,(r_1 + B_1 r_2) - D_1(r_1 - B_1 r_2)\right]\sin\xi b + EI\frac{m\pi}{a}\left[B_1\cos\xi b + \right. \qquad (A.16)$$

$$\left.\left.\tanh\eta b\sin\xi b\right]\right\} - q(x) = 0$$

This gives the deflected surface of the plate on substituting back into the expression for w.

NOTATION

a	length of flange plate
2b	width of flange plate
$2b_e$	effective width of flange plate

t	thickness of flange plate
D	depth of stiffener
B	spacing of stiffeners
T	thickness of stiffener
E	Young's modulus
ν	Poisson's ratio
w	lateral deflection
D_x	flexural rigidity in x-direction
D_y	flexural rigidity in y-direction
H	effective torsional rigidity
J	torsional constant for a stiffener
M_x	moment in x-direction
M_y	moment in y-direction
M	total applied bending moment at a section
$q(x)$	loading applied to main girder in x-direction
I	second moment of area of web (main girder)
I_s	second moment of area of stiffener about centroid of plate/ stiffener section
h	distance from plate mid-plane to centroid of plate/stiffener section
A_1, A_2	constants of integraton
β	effective width ratio = b_e/b

ACKNOWLEDGEMENT

The authors would like to acknowledge the financial assistance of the Science and Engineering Research Council of Great Britain.

REFERENCES

1. LAMAS, A.R.G, FRIEZE, P.A. and DOWLING, P.J. Interaction between shear lag and stiffener-induced buckling in steel box girders. Instability and Plastic Collapse of Steel Structures, L.J. Morris ed., 1983.

2. LAMAS, A.R.G. Influence of shear lag on the collapse of wide flange girders. Ph.D. Thesis, University of London, Imperial College, June 1979.

3. CHAPMAN, J.C., DOWLING, P.J., LIM, P.T.K. and BILLINGTON, C.J. The structural behaviour of steel and concrete box girder bridges. The Structural Engineer, March 1971, No. 3, volume 49.